



Box-Behnken design for development and characterization of nanostructured chitosan-based nanoparticles containing sulfasalazine for the treatment of ulcerative colitis

Ganesh Narayan Sharma^{*1}, Praveen Kumar C H², Birendra Shrivastava³, Kumar B⁴, Arindam Chatterjee⁵

¹Department of Pharmacology, School of Pharmaceutical Sciences, Jaipur National University, Jagatpura-302017, Jaipur, India

²Research Scholar, School of Pharmaceutical Sciences, Jaipur National University, Jagatpura-302017, Jaipur, India

³School of Pharmaceutical Sciences, Jaipur National University, Jagatpura-302017, Jaipur, India

⁴Department of Pharmaceutics, Ratnam Institute of Pharmacy, Muthukur (M), Nellore -524346, Andhra Pradesh, India

⁵Department of Pharmaceutics, School of Pharmaceutical Sciences, Jaipur National University, Jagatpura-302017, Jaipur, India

Article History:

Received on: 05.08.2019

Revised on: 16.11.2019

Accepted on: 22.11.2019

Keywords:

Sulfasalazine,
Chitosan,
Ulcerative colitis,
Nanoparticles,
Box-Behnken design

ABSTRACT

The present research was designed to improve the permeability of sulfasalazine by loading it into chitosan nanoparticles using the ionic gelation method. The process parameters were screened and optimized through Box-Behnken design. 13 formulations containing sulfasalazine chitosan-based nanoparticles (SCSNPs) were optimized using particle size, zeta potential, and % encapsulation efficiency as responses. The effect of every factor on responses was statistically analyzed using ANOVA and p-Value, and the correlation coefficient of all the responses was found to be >0.99 and >0.96 for optimized CSNPs and optimized SCSNPs respectively with $p < 0.05$. From the predicted and observed values of responses, the optimized formulation (SCSNPs) has a particle size of 261 ± 3.06 nm, with an encapsulation efficiency of $81.3 \pm 5.3\%$. Morphology of the particles using scanning electron microscopy reveals nearly spherical shaped particles with a zeta potential of $+41.4 \pm 0.5$ mV. In-vitro studies acknowledge that sulfasalazine was released in a sustained manner for about 24 hrs in simulated colonic fluid pH 7 and phosphate buffer pH 7.4, when compared to a simulated colonic fluid at fed (pH 6) and fasted state (pH 7.8).



*Corresponding Author

Name: Ganesh Narayan Sharma

Phone: +917791832857

Email: ganeshmph@gmail.com

ISSN: 0975-7538

DOI: <https://doi.org/10.26452/ijrps.v11i1.1855>

Production and Hosted by

IJRPS | www.ijrps.com

© 2020 | All rights reserved.

INTRODUCTION

Sulfasalazine is an aminosalicylate used in the short term and long term treatment of ulcerative colitis (UC) (Taylor and Irving, 2011; Isaacs *et al.*, 2005). Sulfasalazine is BCS class-IV drug with least permeability and solubility and have many challenges for the researchers working on novel targeted drug delivery system (Lindenberg *et al.*, 2004). Many researchers found that sulfasalazine has a maximum percentage of remission in UC when compared to Crohn's disease, which were grouped together as

inflammatory bowel disease (Schroeder *et al.*, 1987; Sninsky, 1991; Hanauer, 1996).

Hence in the present research, a safe and effective dosage form was prepared to target sulfasalazine into the colon. For this intention, chitosan was selected as a polymer due to its biodegradability, biocompatibility, and ability to sustain the drug release in colonic pH (Nagpal *et al.*, 2010). The presence of primary amine at the C-2 position of glucosamine residue made chitosan as an important polysaccharide for the fabrication of functional drug delivery. The ability of chitosan to release the drug in a sustained manner is due to deprotonation of amines that undergo interpolymer associations leading to film and gel formation (Younes and Rinaudo, 2015; Yi *et al.*, 2005). Ionic gelation method was used in the fabrication of SCSNPs due to the avoidance of organic solvents with less shear forces (Tiyaboonchai, 2003). From the literature, it was found that sulfasalazine nanoparticles were prepared using albumin (Olaitan *et al.*, 2019) mixed alginate-N,O-carboxymethyl chitosan (Tavakol *et al.*, 2013), polymer-coated mesoporous silica nanoparticles (Popova *et al.*, 2018), etc.

The present research was accomplished to optimize and characterize chitosan-based sulfasalazine nanoparticles using Box-Behnken design. The prepared chitosan-based sulfasalazine nanoparticles were filled in capsules, which were further coated with pH-sensitive polymers like cellulose acetate phthalate and eudragit-S 100 using polyethylene glycol-300 as a plasticizer.

MATERIALS AND METHODS

Sulfasalazine was kindly gifted by SP Accure Labs, Hyderabad. Chitosan, Tripolyphosphate (TPP), and Phosphotidylcholine was purchased from Sigma Aldrich, Mumbai. Eudragit S-100, Cellulose acetate phthalate was obtained from Drugs India, Hyderabad. Tris and Bovine serum albumin from Thermo Fisher Scientific, Hyderabad. Sodium phosphate dibasic, Sodium hydroxide, Dichloromethane, Potassium phosphate monobasic was obtained from New Himalaya Scientific Company, Nellore. All the chemicals used were of analytical grade.

Fabrication of blank chitosan nanoparticles using ionic gelation method

Chitosan (CS) solutions were prepared by dissolving chitosan in aqueous acetic acid, according to the formulation of Table 2. Tripolyphosphate (TPP) aqueous solutions were prepared according to the stated quantities and added dropwise to the chitosan solutions under stirring at 400rpm for 100

minutes using IKA stirrer for the preparation of chitosan nanoparticles (CSNPs). If necessary, pH was adjusted to 4.5 using Mettler Toledo pH meter with 1M aqueous sodium hydroxide solution in order to neutralize the excess acid. Then CS-TPP suspension was ultrasonicated using PCI analytics ultrasonicator for 5 minutes to produce CSNPs with controlled sizes. CS-TPP suspension was vacuum filtered using a Millipore vacuum pump, and produced CSNPs were dried.

The technique was optimized by Design-Expert software using Box Behnken design (BBD) with 13 run, 3-factor, 3-level, as shown in Table 1. The design is suitable for investigating the quadratic response surface and constructing a second-order polynomial model. The dependent and independent variables with actual values were shown in the table. Temperature (35°C), pH (4.5), and stirring speed (600rpm) was considered as constant variables for the preparation of chitosan-based nanoparticles.

Fabrication of sulfasalazine loaded chitosan nanoparticles using ionic gelation method

By using the optimized factors of blank CSNPs, formulation parameters for the preparation of sulfasalazine CSNPs were identified and screened through BBD. Thirteen batches were prepared according to the design, as shown in Table 4 and evaluated for particle size, zeta potential, and entrapment efficiency (%EE). The dependent and independent variables were shown in Table 3. The concentrations of chitosan, tripolyphosphate, and acetic acid was kept constant as per the optimized factors of blank CSNPs. The method of preparation is the same as the preparation of blank CSNPs.

Morphology of CSNPs and SCSNPs

Morphology and shape analysis of optimized formulations were evaluated using SEM (Hitachi S-4300 Microscope). The formulations were placed on the double-sided adhesive carbon tabs and adhered to aluminium stubs coated with gold/palladium alloy using the Emscope sputter coating system at 20μA for 1 minute under argon gas. An electronic beam at an accelerating voltage of 5-10kV was used at a working distance of 13-15mm. Using similar conditions, images were captured at several magnifications (Goldstein *et al.*, 2003).

Particle size and (Poly Dispersity Index) PDI

Freshly prepared nanoparticles of sulfasalazine were diluted 200 times with deionized water and measured the particle size, PDI, and zeta potential using Malvern zeta sizer nano (ZS90). The average particle size was measured by dynamic light scattering at an angle of 90°. The properties of dispersion

Table 1: Variables with coded and actual values for Box behnken design (Formulation- Blank CSNPs)

Independent variables	Low	Medium	High
Coded Values	(-1)	(0)	(1)
A = Chitosan (mg/ml)	2	3.5	5
B = Tripolyphosphate (mg/ml)	0.5	1.25	2
C = Acetic acid (mg/ml)	0.2	0.5	0.8
Dependent variables Constrains			
Y1 = Particle size (nm): Goal – Minimize			
Y2 = Zeta potential (mV): Goal – In range			
Y3 = Poly dispersity Index: Goal – Minimize			

Table 2: Formulations showing factors optimized by Box Behnken design (Formulation- Blank CSNPs)

Formulation Code	Factor-1 Chitosan (mg/ml)	Factor-2 Tripolyphosphate (mg/ml)	Factor-3 Acetic acid (mg/ml)
CNI -1	5	1.25	0.8
CNI -2	2	2	0.5
CNI -3	3.5	1.25	0.5
CNI -4	2	1.25	0.2
CNI -5	2	1.25	0.8
CNI -6	3.5	2	0.8
CNI -7	3.5	2	0.2
CNI -8	5	0.5	0.5
CNI -9	3.5	0.5	0.8
CNI -10	3.5	0.5	0.2
CNI -11	5	2	0.5
CNI -12	5	1.25	0.2
CNI -13	2	0.5	0.5

Table 3: Variables with coded and actual values for Box Behnken design (Formulation-Sulfasalazine CSNPs)

Independent variables	Low	Medium	High
Coded Values	(-1)	(0)	(1)
A= Sulfasalazine (mg/ml)	1	1.5	2
B=Stirring Speed (rpm)	400	600	800
C= Temperature (0C)	10	22.5	35
Dependent variables Constrains			
Y1 = Particle size (nm) : Goal – Minimize			
Y2 = Zeta potential (mV): Goal – Maximize			
Y3 = % EE: Goal – Maximize			

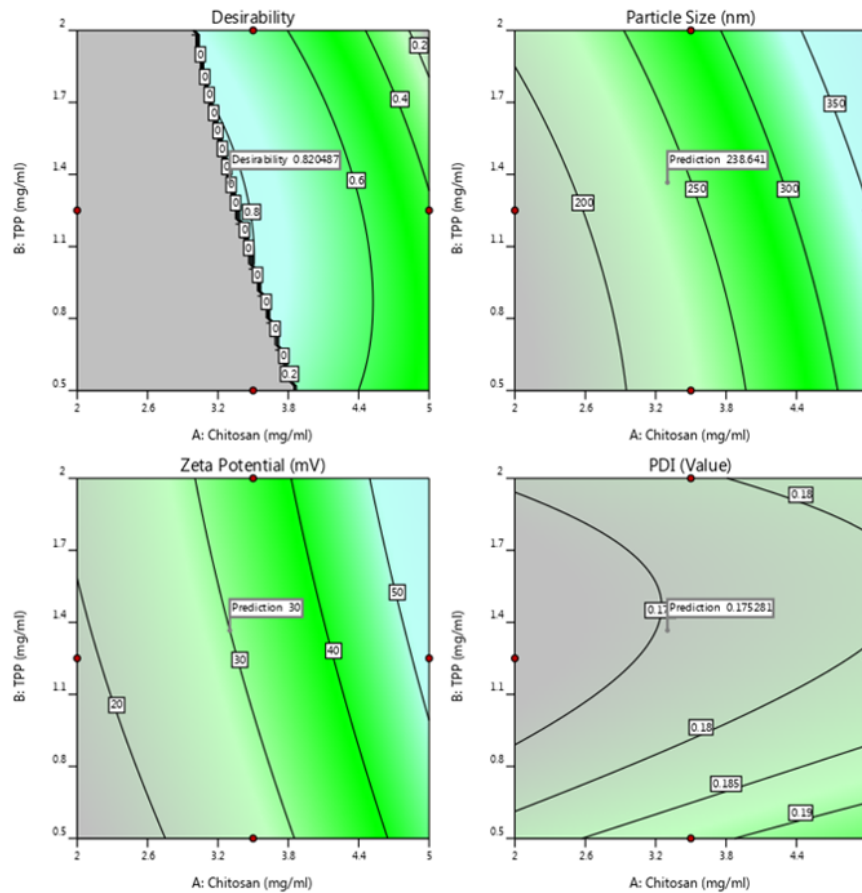


Figure 1: 2D Response surface Contour plots showing desirability between factors and responses (CSNPs)

Table 4: Formulations showing factors optimized by Box Behnken design (Formulation-Sulfasalazine CSNPs)

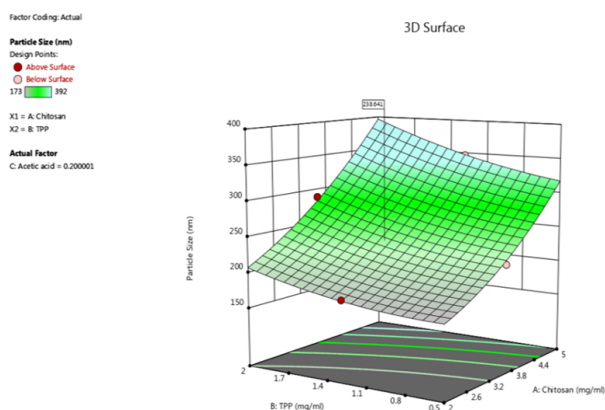
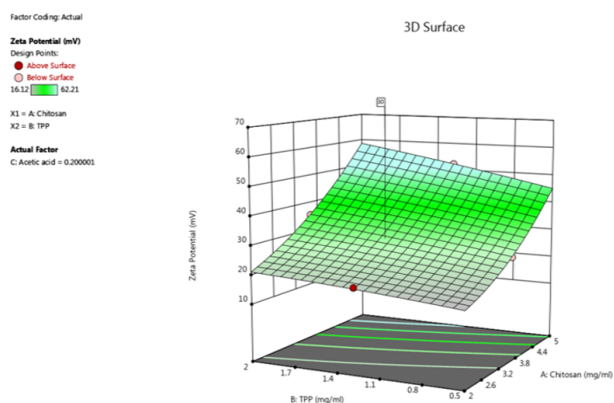
Formulation Code	Factor-1 Sulfasalazine (mg/ml)	Factor-2 Stirring Speed (rpm)	Factor-3 Temperature (0C)
SCSNP -1	2	600	10
SCSNP -2	1	600	35
SCSNP -3	2	800	22.5
SCSNP -4	1.5	400	10
SCSNP -5	1.5	600	22.5
SCSNP -6	1	600	10
SCSNP -7	1.5	800	10
SCSNP -8	2	400	22.5
SCSNP -9	1.5	800	35
SCSNP -10	1	400	22.5
SCSNP -11	2	600	35
SCSNP -12	1	800	22.5
SCSNP -13	1.5	400	35

Table 5: Optimization of blank chitosan based nanoparticles using ionic gelation technique: (Formulation -Blank CSNPs) n=3

Formulation Code	Response-1 (Y1) Particle size (nm)	Response -2 (Y2) Zeta potential (mV)	Response -3 (Y3) PDI
CNI -1	359±6.31	59.19±0.69	0.231±0.003
CNI -2	196±4.34	21.13±1.02	0.186±0.002
CNI -3	245±6.45	33.43±0.53	0.193±0.001
CNI -4	180±7.32	19.32±0.49	0.173±0.004
CNI -5	183±8.12	20.11±1.16	0.197±0.002
CNI -6	293±9.11	39.61±0.59	0.216±0.004
CNI -7	289±8.13	35.51±0.89	0.177±0.003
CNI -8	329±6.21	49.12±1.32	0.217±0.002
CNI -9	231±6.34	31.21±1.11	0.232±0.003
CNI -10	219±7.22	26.17±1.34	0.189±0.003
CNI -11	392±3.45.	62.21±0.67	0.206±0.002
CNI -12	347±5.45	52.31±0.78	0.181±0.006
CNI -13	173±6.34	16.12±0.65	0.192±0.003

Table 6: Summary of regression analysis of the responses (CSNPs)

Quadratic model	R2	Adjusted R2	SD	Adequate Pre- cision	p-value
Response-1 Particle size (nm)	0.99	0.98	9.57	27.19	0.0020
Response -2 Zeta potential (mV)	0.99	0.99	0.51	98.00	0.0001
Response -3 PDI	0.99	0.97	0.0028	24.36	0.0342

**Figure 2: 3D Response surface plots showing factors with particle size (CSNPs)****Figure 3: 3D Response surface plots showing factors with zeta potential (CSNPs)**

and stability of nanoparticles was also measured using the same instrument. All the measurements were done in triplicate at 25°C (Olaitan *et al.*, 2019; Kaur *et al.*, 2011; Shevchenko *et al.*, 2006; Dubes *et al.*, 2003).

Entrapment efficiency (%EE)

The amount of sulfasalazine encapsulated in the

nanoparticles were determined by separating the free drug using ultracentrifugation (Remi centrifuge). The formulations were centrifuged at around 18000rpm for 40min. The supernatant was collected, and the concentration of sulfasalazine incorporated in the formulations was analyzed separately using Shimadzu UV Spectrophotometer at

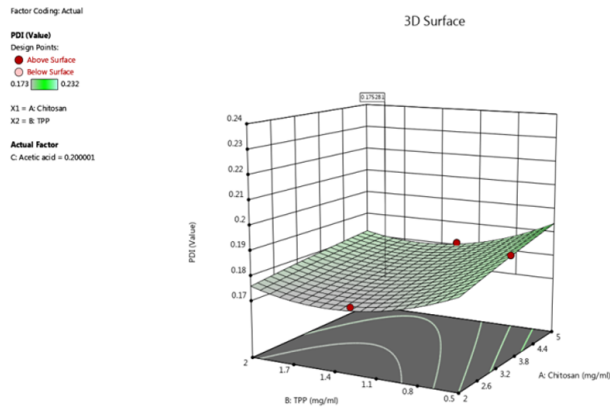


Figure 4: 3D Response surface plots showing factors with PDI (Polydispersity index) (CSNPs)

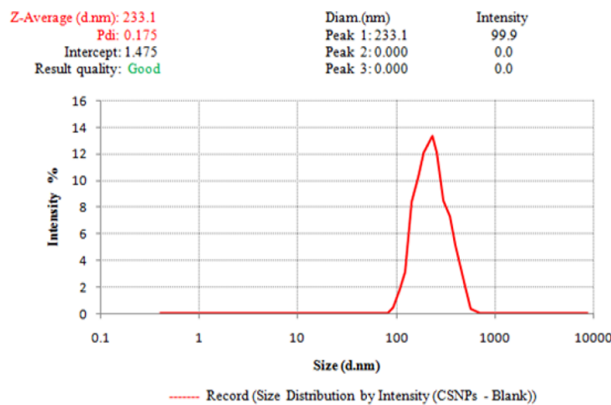


Figure 5: Average particle size of Optimized formulation (blank CSNPs)

359 nm (Patel and Gajra, 2016; Piacentini, 2016).

$$\%EE = (S_a - S_b) / S_a * 100$$

S_a = Total amount of drug in the system, S_b = Amount of drug in supernatant after centrifugation

FT-IR studies for optimized formulation

Cross-linking reaction between a phosphoric group of tripolyphosphate (TPP) and an amino group of chitosan was analyzed to confirm using Perkin Elmer spotlight 200i ft-ir. Homogenously dried formulation was used to prepare the KBr pellet, where the powder was compressed under vacuum using a round flat face punch. Samples were scanned from about 4000-400 cm^{-1} (Ray et al., 2010).

Powder X-ray Diffraction (PXRD)

Information regarding crystal lattice arrangements and the degree of crystallinity of optimized formulations were analyzed using PXRD. In order to analyze the physical state, PXRD spectra of dried nanoparticles were recorded at room temperature using Arex X-ray diffractometer with a voltage of 3Kv, 5Ma current with a scanning speed of 40/min. Samples were scanned from 0-600 (2θ) range with a step interval

of 0.1 seconds (Qi et al., 2004).

In-Vitro Drug release

Drug release was performed in-vitro using a dialysis bag method. Dialysis bags were soaked in deionized water overnight prior to the experiment. Nanoparticle dispersion of 2ml is placed in the dialysis bag of 2000 Da and fixed two ends with the help of clamps. The bags were transferred into 250ml phosphate buffer pH 7.4 and in simulated colonic fluid (Fed and Fasted state) kept at $35 \pm 0.5^\circ\text{C}$ for the determination of drug release. Samples were withdrawn at specified time intervals for about 24 Hrs. At pre-determined time intervals, 1ml of the sample was withdrawn by adding the fresh buffer/fresh simulated colonic fluid. The samples were analyzed using UV spectrophotometry at 359nm. All the measurements were done in triplicate. By using various kinetic models, the mechanism of drug release was noted based on R^2 and 'n' value (Dash et al., 2010).

RESULTS AND DISCUSSION

Statistical analysis (Box-Behnken design)

The results of Box-Behnken design were analyzed, and the utility of this statistical design resulted in providing considerable information to optimize the formulation. All the responses were fitted to the quadratic model, and compatibility of the model was verified by ANOVA, lack of fit, and co-efficient of determination (R^2). To optimize the responses, every response should be interconnected with each other, and a most supportive zone must be required for every response to exclude bias. Desirability function was supported by many kinds of literature to optimize the multiple responses (Marasini et al., 2012; Ferreira et al., 2007).

Blank chitosan nanoparticles were formulated to optimize the concentration of chitosan, TPP, and acetic acid based on the dependent variables like particle size, zeta potential, and polydispersity index (PDI). The results for the responses were shown in Table 5. With an increase in the concentration of chitosan and TPP, particle size and zeta potential was increased and vice versa. PDI increased linearly with increase in the concentration of acetic acid which was in acceptance according to the literature (Gan et al., 2005; Grenha et al., 2005; Liu and Gao, 2009). P-Values for the responses y_1 , y_2 , y_3 was found to be 0.002, 0.001, 0.034. Hence the quadratic model is best fitted for all the responses with $p < 0.05$. Table 6 shows a summary of the regression analysis of all the responses. Polynomial Equations (1), (2) and (3) for Y_1 , Y_2 , Y_3 , explains the significant model terms with $p < 0.05$. The variables

Table 7: Comparison of predicted and observed values of blank CSNPs

Confirmation Location	Chitosan (A)	TPP (B)	Acetic acid (C)	
	3.30	1.36	0.2	
Response	Predicted Value	Observed value	Residuals	*Bias %
Particle size (nm)	238.64	233±13.3	-5.64	2.42
Zeta potential (mV)	30	32.01±3.11	2.1	-6.27
PDI	0.175	0.171±0.004	-0.004	2.33

Table 8: Optimization of sulfasalazine chitosan based nanoparticles using ionic gelation technique: (Formulation –Sulfasalazine CSNPs)

Formulation Code	Response-1 (Y1) Particle size (nm)	Response -2 (Y2) Zeta potential (mV)	Response -3 (Y3) % EE
SCSNP -1	354±9.34	33.63±2.31	81.93±1.78
SCSNP -2	239±8.13	33.56±3.22	74.13±1.30
SCSNP -3	319±9.54	24.13±2.89	67.89±1.34
SCSNP -4	283±8.32	34.59±1.86	80.11±2.31
SCSNP -5	289±9.15	43.21±1.79	84.17±1.45
SCSNP -6	253±8.18	31.39±2.78	76.15±1.32
SCSNP -7	316±7.21	23.16±3.41	66.73±1.31
SCSNP -8	299±4.32	41.16±3.33	80.02±1.36
SCSNP -9	293±8.34	22.45±3.56	64.19±1.34
SCSNP -10	243±6.33	36.32±2.78	71.19±1.56
SCSNP -11	286±7.82	35.23±3.54	80.67±2.31
SCSNP -12	240±3.19	21.31±3.36	63.13±2.56
SCSNP -13	276±6.14	33.12±2.78	78.16±3.12

Table 9: Summary of regression analysis of the responses (Sulfasalazine CSNPs)

Quadratic model	R2	Adjusted R2	SD	Adequate Precision	p-value
Response-1 Particle size (nm)	0.96	0.86	12.85	9.63	0.0472
Response -2 Zeta potential (mV)	0.96	0.87	2.49	10.10	0.0398
Response -3 % EE	0.98	0.95	1.50	16.50	0.0088

Table 10: Comparison of predicted and observed values of SCSNPs

Confirmation Location	Sulfasalazine (mg/ml)	Stirring speed (RPM)	Temperature (0C)	
	1.29	525.16	23.14	
Response	Predicted Value	Observed value	Residuals	*Bias %
Particle size (nm)	269.61	261±3.06	-8	3.29
Zeta potential (mV)	43.21	41.4±0.5	-1.81	4.37
% EE	82.83	81.3±5.3	-1.53	1.88

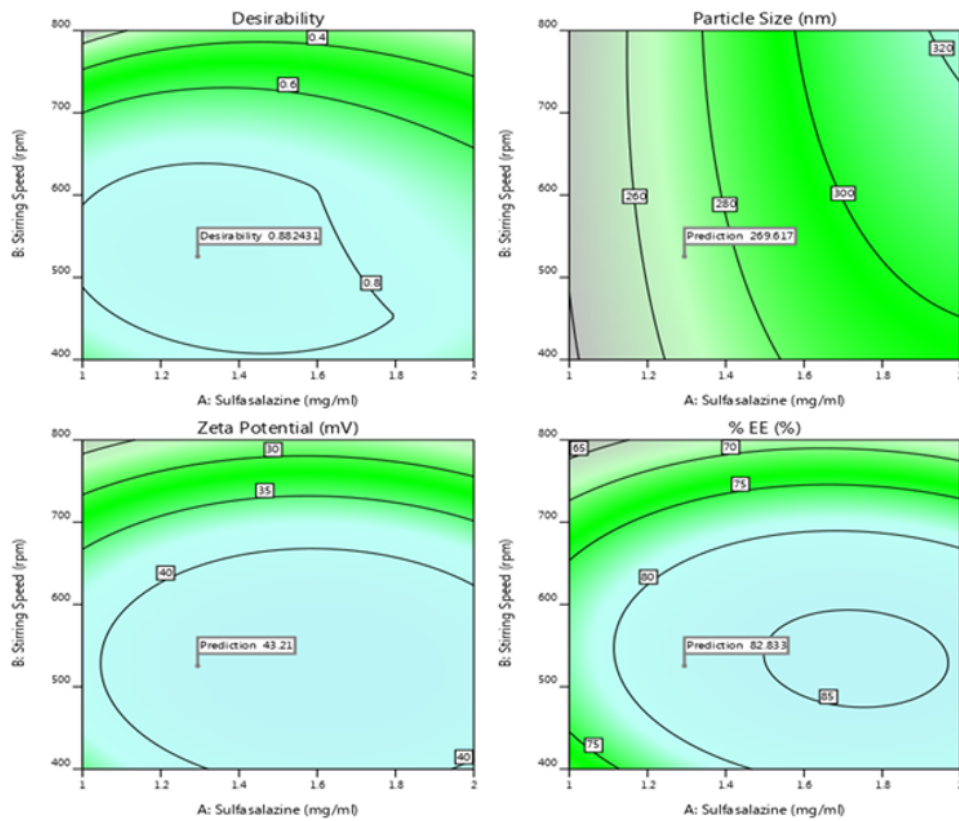


Figure 6: 2D Response surface Contour plots showing desirability between factors and responses (Sulfasalazine CSNPs)

Table 11: In-Vitro Drug release studies of sulfasalazine CSNPs (n=3)

Time (Hrs)	% Drug release (phosphate buffer pH 7.4)	% Drug release simulated colonic fluid - pH 7	% Drug release simulated colonic fluid (Fed State) - pH 6	% Drug release simulated colonic fluid (Fasted State) - pH 7.8
1	15.15±1.35	15.20±0.82	17.67±1.39	14.10±0.82
2	22.70±1.60	21.67±1.50	24.20±1.05	17.93±0.55
3	25.70±1.40	25.10±1.06	37.30±1.73	23.17±1.33
4	30.10±1.50	30.20±1.49	45.83±2.28	28.67±0.81
5	34.70±0.40	36.10±0.44	50.53±1.30	33.40±1.06
6	40.80±1.70	40.10±0.92	58.30±0.10	38.23±0.64
7	44.75±2.15	43.77±0.74	62.87±1.21	42.13±0.40
8	49.65±0.55	50.67±1.25	70.73±1.46	47.13±1.01
9	56.90±0.50	56.33±1.79	77.50±1.64	52.10±0.66
10	61.10±1.20	60.73±0.72	81.93±0.64	57.83±0.67
11	65.35±0.55	65.87±1.21	89.97±1.17	62.60±1.42
12	70.10±1.20	69.83±0.50	99.03±0.80	65.30±0.46
16	82.60±0.70	82.13±1.53	-	79.74±1.38
24	99.95±1.45	99.70±0.72	-	91.40±0.96

Table 12: Drug release kinetics of optimized SCSNPs

SCSNPs	Zero (R2)	Order	First Order (R2)	Higuchi (R2)	Korsmeyer Peppas (R2)	(n)
SCSNPs - PBS (pH 7.4)	0.94		0.74	0.98	0.98	0.62
SCSNPs - SCF FED (pH 6)	0.98		0.72	0.97	0.99	0.69
SCSNPs - SCF FASTED (pH 7.8)	0.93		0.98	0.97	0.98	0.65
SCSNPs - SCF (pH 7)	0.94		0.80	0.98	0.98	0.63

with negative values represent negative effects on responses. Based on the desirability function, interaction effects between two factors and confirmation location was predicted using 2D contour and 3D response surface graphs shown in Table 7 and Figures 1, 2, 3 and 4. Among the responses, Y_1 and Y_3 were set in minimize, whereas Y_2 in range. Confirmation location for the optimized formulation was achieved at $A = 3.30$ mg/ml, $B = 1.36$ mg/ml, $C = 0.2$ mg/ml with $Y_1 = 238.64$ nm, $Y_2 = 30$ mV and $Y_3 = 0.175$. The average particle size of the optimized CSNPs was given in Figure 5. Observed values for the confirmation location was found to be close to the predicted values indicating that Box Behnken Design can be considered as the best tool in formulating sulfasalazine chitosan nanoparticles.

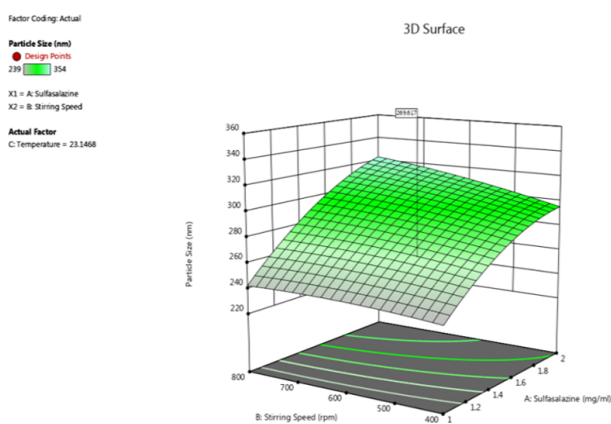


Figure 7: 3D Response surface plots showing factors with particle size (SCSNPs)

Polynomial equations with intercept and coded factors (CSNPs)

$$\begin{aligned}
 Y_1 = & +245 + 86.87A(P < 0.05) + 27.25B \\
 & (P < 0.05) + 3.87C(P > 0.05) + 10AB \\
 & (P > 0.05) + 2.25AC(P > 0.05) - 2BC \\
 & (P > 0.05) + 18.37A^2(P < 0.05) + 9.12B^2 \\
 & (P > 0.05) + 3.87C^2(P > 0.05).
 \end{aligned}
 \tag{1}$$

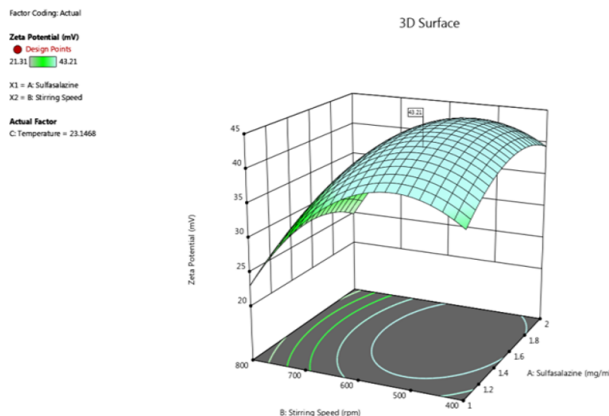


Figure 8: 3D Response surface plots showing factors with zeta potential (SCSNPs)

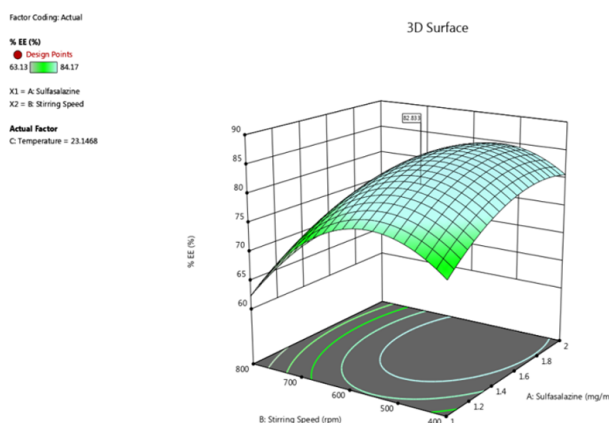


Figure 9: 3D Response surface plots showing factors with encapsulation efficiency (SCSNPs)

$$\begin{aligned}
 Y_2 = & +33.43 + 18.26A(P < 0.05) + 4.48B \\
 & (P < 0.05) + 2.10C(P < 0.05) + 2.02AB \\
 & (P < 0.05) + 1.52AC(P < 0.05) - 0.23BC \\
 & (P > 0.05) + 4.16A^2(P < 0.05) - 0.44B^2 \\
 & (P > 0.05) + 0.14C^2(P > 0.05).
 \end{aligned}
 \tag{2}$$

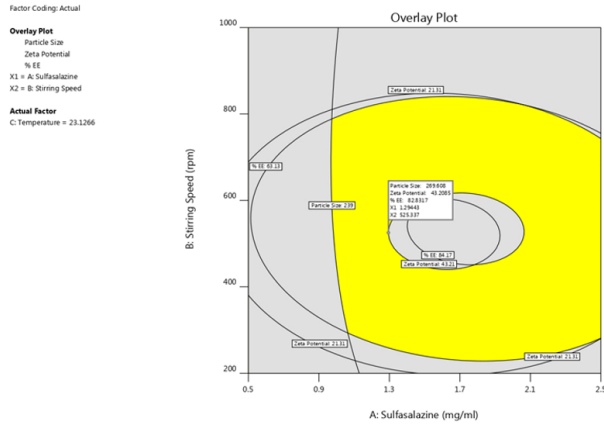


Figure 10: Overlay contour plot for Sulfasalazine CSNPs (SCSNPs)

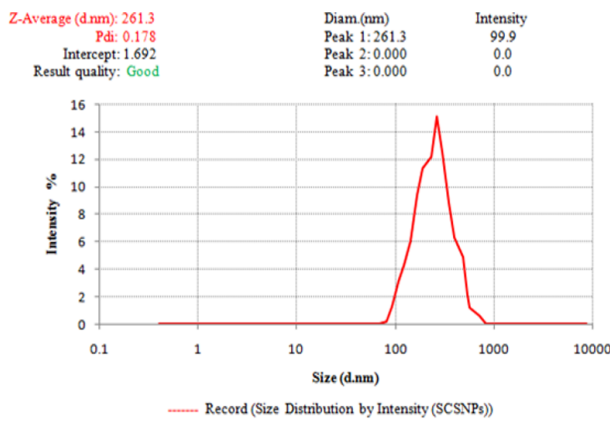


Figure 11: Average particle size of optimized SCSNPs

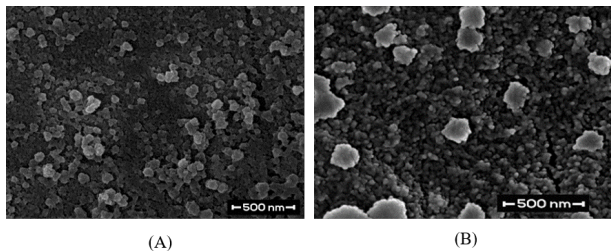


Figure 12: SEM photographs of A) Optimized CSNPs, B) Optimized SCSNPs

$$Y_3 = +0.19 + 0.01A(P < 0.05) - 0.00B(P < 0.05) + 0.01C(P < 0.05) - 0.00AB(P > 0.05) + 0.00AC(P < 0.05) - 0.00BC(P > 0.05) - 0.00A^2(P > 0.05) + 0.00B^2(P < 0.05) + 0.00C^2(P > 0.05). \quad (3)$$

SCSNPs were formulated to optimize the concentration of sulfasalazine, stirring speed, and temperature based on the dependent variables like particle size, zeta potential, and encapsulation efficiency. Table 8 shows the results for responses. p-Values for the responses y_1 , y_2 , y_3 was found to be 0.047,

0.039, 0.008. Hence the quadratic model is best fitted for all the responses with $p < 0.05$. Table 9 shows a summary of the regression analysis of all the responses. Based on the desirability function, interaction effects between two factors and confirmation location was predicted using 2D contour and 3D response surface graphs shown in Table 10 and Figures 6, 7, 8, 9 and 10. Among the responses, Y_2 and Y_3 were set in maximize, whereas Y_1 in minimize. Confirmation location for the optimized formulation was achieved at $A = 1.29$ mg/ml, $B = 525.16$ rpm, $C = 23.14^\circ\text{C}$ with $Y_1 = 269.61$ nm, $Y_2 = 43.21$ mV and $Y_3 = 82.83\%$ (Desirability - 0.88). Overlay contour plot shown in Figure 10 explains the most supportive zone for all the responses. Observed values were found to be very close to the predicted values of confirmation location, indicating the best optimization results using Box Behnken Design.

Particle Size

There is an increase in particle size with increasing the concentration of sulfasalazine. Particle size was found to be increased with an increase in stirring speed upto 600rpm and decreased thereafter, which may be due to the prevalence of high shearing rates that destroys the repulsive forces leading to aggregation (Tsai et al., 2008; Carvalho et al., 2009). Particle size decreased linearly with an increase in temperature, which is shown in 3D response surface graphs (Figure 7). Polynomial equation with intercept and coded factors is as follows,

$$Y_1 = +289 + 35.37A(P < 0.05) + 8.37B(P > 0.05) - 14C(P < 0.05) + 5.75AB(P > 0.05) - 13.5AC(P > 0.05) - 4BC(P > 0.05) - 11.37A^2(P > 0.05) - 2.37B^2(P > 0.05) + 5.377C^2(P > 0.05). \quad (4)$$

From the Equation (4), independent variables like A and C was found to be significant as the p-value is less than 0.05. The observed value of particle size for the confirmation location was found to be 261 ± 3.06 , and the results were given in Table 10 and Figure 11.

% Encapsulation efficiency (EE)

%EE of all the SCSNPs ranged from 63.13 ± 2.56 to $84.17 \pm 1.45\%$. Polynomial equation with intercept and coded factors is as follows,

$$Y_3 = +84.17 + 3.23A(P < 0.05) - 5.94B(P < 0.05) - 0.97C(P > 0.05) - 1.0AB(P > 0.05) + 0.19AC(P > 0.05) - 0.14BC(P > 0.05) - 3.8A^2(P < 0.05) - 9.7B^2(P < 0.05) - 2.1C^2(P > 0.05). \quad (5)$$

From Equation (5), the independent variables like A, B, A^2 , and B^2 was found to be significant as the p-value is less than 0.05. Encapsulation efficiency was

found to be increased up to 1.5mg/ml concentration of sulfasalazine and decreased thereafter. Further increase in sulfasalazine concentration leads to a decrease in % EE, which may be due to the precipitation of chitosan molecules in the dispersion. %EE was found to be increased up to 600 rpm and decreased thereafter, which may be due to the prevalence of high shearing rates that destroys the repulsive forces leading to aggregation (Tsai *et al.*, 2008; Carvalho *et al.*, 2009). These results were clearly shown in the 3D response surface graph, Figure 9. Observed % EE of the optimized batch was found to be 81.3 ± 5.3 , with particle size 261 ± 3.06 .

Zeta potential

Zeta potential of all SCSNPs ranged from 21.31 ± 3.36 to 43.21 ± 1.79 mV. Polynomial equation with intercept and coded factors is as follows,

$$Y_2 = +43.21 + 1.244A(P > 0.05) - 6.76B(P < 0.05) + 0.19C(P > 0.05) + 0.5AB(P > 0.05) + 0.14AC(P > 0.05) + 0.19BC(P > 0.05) - 3.6A^2(P > 0.05) - 8.8B^2(P < 0.05) - 6.0C^2(P < 0.05). \quad (6)$$

From Equation (6), independent variables like B, B², and C² was found to be significant as the p-value is less than 0.05. Zeta potential was mainly affected by stirring speed and temperature. At higher speeds and temperature, a decrease in the viscosity of chitosan leads to structural instability, thereby decreasing zeta potential (Rampino *et al.*, 2013). The observed value of zeta potential for the confirmation location was found to be $+41.4 \pm 0.5$. This positive surface charge leads to interaction with mucin and has the characteristics of mucoadhesion (Hong *et al.*, 2017).

Morphology

Scanning electron microscopy reveals that there is an increase in the particle size of SCSNPs when compared to CSNPs. From the micrographs (Figure 12), it was evident that particles were rough in texture with a nearly spherical shape.

FT-IR Spectroscopy

Characteristic peaks for sulfasalazine, optimized blank CSNPs, and optimized SCSNPs were shown in Figure 13. Characteristic peaks for chitosan at 3361 cm^{-1} (N-H and O-H stretch) shifted to a higher number of 3420 cm^{-1} with broadband in CSNPs. Other peaks at 1658 cm^{-1} (C=O) and 1577 cm^{-1} (NH₂ bending) shifted to lower numbers of 1628 cm^{-1} and 1560 cm^{-1} , respectively (Papadimitriou *et al.*, 2008; Vino *et al.*, 2012). These shifts may be due to the interaction between chitosan and TPP. CSNPs showed new characteristic peaks

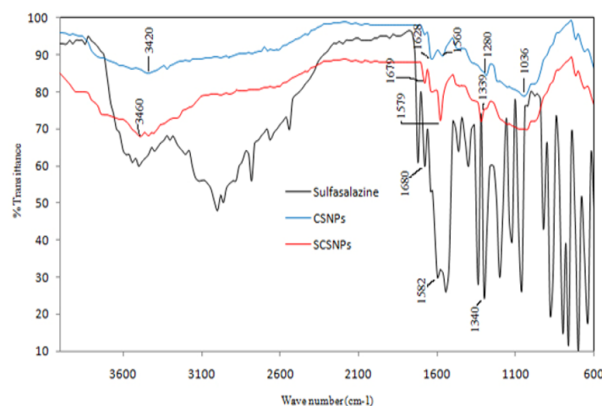


Figure 13: FT-IR of Sulfasalazine (Pure Drug), Optimized blank chitosan nanoparticles (CSNPs), Optimized sulfasalazine nanoparticles (SCSNPs)

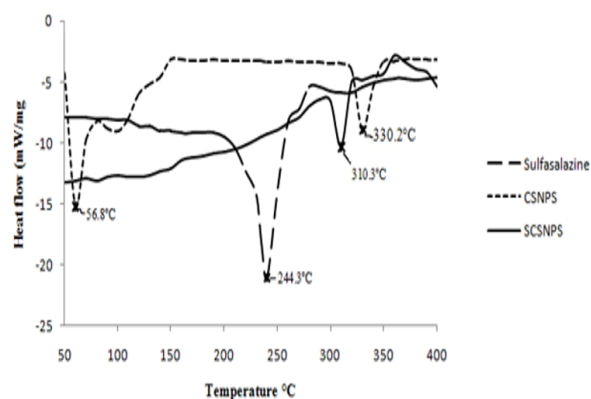


Figure 14: DSC of Sulfasalazine (Pure Drug), Blank chitosan nanoparticles (CSNPs), Optimized sulfasalazine nanoparticles (SCSNPs)

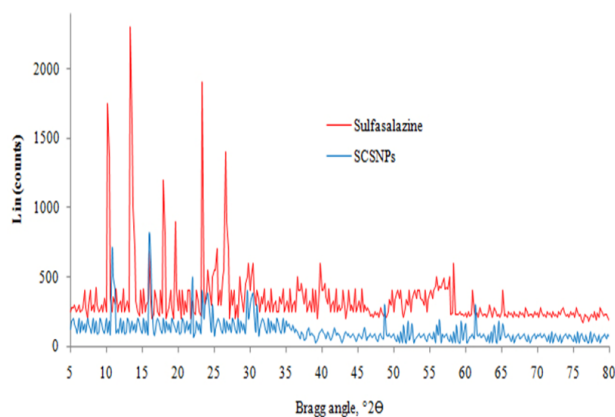


Figure 15: PXRD of Sulfasalazine and optimized sulfasalazine nanoparticles (SCSNPs)

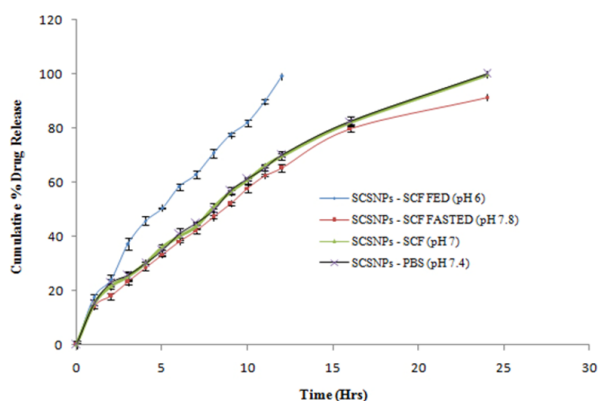


Figure 16: Cumulative % drug release of optimized sulfasalazine nanoparticles (SCSNPs) in various fluids (SCF-Simulated Colonic Fluid, PBS – Phosphate buffer)

of tripolyphosphate at 1280 cm^{-1} (P=O stretching) and 1036 cm^{-1} (P-O bending). Characteristic peaks for sulfasalazine at 1340 cm^{-1} (asymmetric stretching mode of SO_2), 1385 cm^{-1} (O-H bending), 1410 cm^{-1} (symmetric stretching mode of COO^-), 1582 cm^{-1} (stretching mode of N=N) slightly shifted to lower wavenumbers in SCSNPs indicating the interactions between chitosan/tripolyphosphate matrix and sulfasalazine (Soliman *et al.*, 2005). Broadband at 3460 cm^{-1} and less intense band at 1339 cm^{-1} reveals the possible interaction between -OH group of sulfasalazine and -NH group of chitosan for hydrogen bonding, and this may be the reason for increased encapsulation efficiency of optimized SCSNPs.

Differential Scanning Calorimetry

The broad endothermic peak was observed at 244.3°C for sulfasalazine, corresponding to its melting point shown in Figure 14. CSNPs experienced two endothermic peaks at 56.8°C and 330.2°C , in relation to evaporation of water and degradation of chitosan, respectively (Kittur *et al.*, 2002; Gazori *et al.*, 2009). The endothermic peak of sulfasalazine was shifted from 244.3°C to 310.3°C in SCSNPs, indicating superior thermal stability of sulfasalazine.

X-Ray diffraction

Powdered X-ray diffraction patterns for pure sulfasalazine and optimized SCSNPs were shown in Figure 15. Pure sulfasalazine showed larger Lin (counts) when compared to optimized SCSNPs. Less intensities of sulfasalazine in SCSNPs indicates that the drug is in disordered crystalline or in amorphous form. This studies indicate the improvement of bioavailability of sulfasalazine in SCSNPs (Wang *et al.*, 2012).

In-Vitro drug release studies

Cumulative drug release for optimized SCSNPs was conducted for 24 hrs in phosphate buffer and simulated colonic fluids (SCF), as shown in Table 11 and Figure 16. Cumulative drug release of sulfasalazine CSNPs in phosphate buffer pH 7.4, SCF pH 7, SCF pH 6 (Fed state), SCF pH 7.8 (Fasted state) was found to be 99.95 ± 1.45 , 99.70 ± 0.72 , 99.03 ± 0.80 and $91.40 \pm 0.96\%$ respectively.

In SCF pH 6 (Fed state), more than 99% of the drug was released within 12 Hrs, which may be due to the solubility of chitosan in acidic and slightly acidic pH (Avadi *et al.*, 2010). In SCF pH 7.8 (Fasted state), drug release was retarded, and only 91.40% of the drug was released in 24 hrs, which may be due to the slow gelling capacity of chitosan at higher pH values (Avadi *et al.*, 2010). From the results, it was found that more than 99% of the drug was released in 24 hrs in phosphate buffer pH 7.4 and SCF pH 7, which was found to be the best when compared to the SCSNPs release in other fluids.

Results were fitted with various kinetic models, as shown in Table 12. Korsmeyer-Peppas was found to be the best-fitted model with the mechanism of drug release as non-fickian diffusion with 'n' value ranging from 0.62-0.69.

CONCLUSIONS

Chitosan nanoparticles containing sulfasalazine was formulated and optimized using Design Expert: Quality by Design (QbD) - software. PXRD and DSC of optimized SCSNPs revealed the improvement of bioavailability and stability by converting its low soluble crystalline forms of sulfasalazine to highly soluble amorphous forms. The encapsulation efficiency of SCSNPs was found to be increased due to the interaction between amine and hydroxyl group of chitosan and sulfasalazine, respectively. Increased encapsulation efficiency made SCSNPs to release the drug for about 24 hrs. Although the drug was released for about 24 hrs in-vitro, the stability of SCSNPs in gastric pH should be improved by coating the nanoparticles using pH-sensitive polymers, thereby targeting the drug release to the colon.

REFERENCES

- Avadi, M. R., Sadeghi, A. M. M., Mohammadpour, N., Abedin, S., Atyabi, F., Dinarvand, R., Rafiee-Tehrani, M. 2010. Preparation and characterization of insulin nanoparticles using chitosan and Arabic gum with ionic gelation method. *Nanomedicine: Nanotechnology, Biology and Medicine*, 6(1):58–63.
- Carvalho, E. L. S., Grenha, A., Remuñán-López, C.,

- Alonso, M. J., Seijo, B. 2009. Chapter 15 Mucosal Delivery of Liposome-Chitosan Nanoparticle Complexes. *Methods in Enzymology*, pages 65015–65016.
- Dash, S., Murthy, P. N., Nath, L., Chowdhury, P. 2010. Kinetic modeling on drug release from controlled drug delivery systems. *Acta Poloniae Pharmaceutica*, 67(3):217–223.
- Dubes, A., Parrot-Lopez, H., Abdelwahed, W., Degobert, G., Fessi, H., Shahgaldian, P., Coleman, A. W. 2003. Scanning electron microscopy and atomic force microscopy imaging of solid lipid nanoparticles derived from amphiphilic cyclodextrins. *European Journal of Pharmaceutics and Biopharmaceutics*, 55(3):20–21.
- Ferreira, S. L. C., Bruns, R. E., Ferreira, H. S., Matos, G. D., David, J. M., Brandão, G. C., Santos, W. N. L. 2007. Box-Behnken design: an alternative for the optimization of analytical methods. *Analytica Chimica Acta*, 597(2):179–186.
- Gan, Q., Wang, T., Cochrane, C., Mccarron, P. 2005. Modulation of surface charge, particle size, and morphological properties of chitosan-TPP nanoparticles intended for gene delivery. *Colloids and Surfaces B: Biointerfaces*, 44(2-3):65–73.
- Gazori, T., Khoshayand, M. R., Azizi, E., Yazdizade, P., Nomani, A., Haririan, I. 2009. Evaluation of Alginate/Chitosan nanoparticles as antisense delivery vector: formulation, optimization, and in vitro characterization. *Carbohydrate Polymers*, 77(3):599–606.
- Goldstein, J., Newbury, D. E., Joy, D. C., Echlin, L. C. E., Lifshin, P., Sawyer, E., Michael, L. 2003. Scanning Electron Microscopy and X-Ray Microanalysis. pages 21–60. 3rd Edn.
- Grenha, A., Seijo, B., Remuñán-López, C. 2005. Microencapsulated chitosan nanoparticles for lung protein delivery. *European Journal of Pharmaceutical Sciences*, 25(4-5):427–437.
- Hanauer, S. B. 1996. An Oral Preparation of Mesalamine as Long-Term Maintenance Therapy for Ulcerative Colitis. *Annals of Internal Medicine*, 124(2).
- Hong, S. C., Yoo, S. Y., Kim, H., Lee, J. 2017. Chitosan-Based Multifunctional Platforms for Local Delivery of Therapeutics. *Marine Drugs*, 15(3).
- Isaacs, K. L., Lewis, J. D., Sandborn, W. J., Sands, B. E., Targan, S. R. 2005. State of the art: IBD therapy and clinical trials in IBD. *Inflammatory bowel diseases*, 11(suppl_1):3–12.
- Kaur, S. P., Rao, R., Hussain, A., Khatkar, S. 2011. Preparation and characterization of rivastigmine loaded chitosan nanoparticles. *Journal of Pharmaceutical Sciences and Research*, 3(5):1227–1232.
- Kittur, F. S., Prashanth, K. V. H., Sankar, K. U., Tharanathan, R. N. 2002. Characterization of chitin, chitosan and their carboxymethyl derivatives by differential scanning calorimetry. *Carbohydrate Polymers*, 49(2):185–193.
- Lindenberg, M., Kopp, S., Dressman, J. B. 2004. Classification of orally administered drugs on the World Health Organization Model List of Essential Medicines according to the biopharmaceutics classification system. *European Journal of Pharmaceutics and Biopharmaceutics*, 58(2):265–278.
- Liu, H., Gao, C. 2009. Preparation and properties of ionically cross-linked chitosan nanoparticles. *Polymers for Advanced Technologies*, 20(7):613–619.
- Marasini, N., Yan, Y. D., Poudel, B. K., Choi, H., Yong, C. S., Kim, J. O. 2012. Development and Optimization of Self-Nanoemulsifying Drug Delivery System with Enhanced Bioavailability by Box-Behnken Design and Desirability Function. *Journal of Pharmaceutical Sciences*, 101(12):4584–4596.
- Nagpal, K., Singh, S. K., Mishra, D. N. 2010. Chitosan nanoparticles: a promising system in novel drug delivery. *Chemical & Pharmaceutical Bulletin*, 58(11):1423–1430.
- Olaitan, V., et al. 2019. Desolvation Conditions for Production of Sulfasalazine Based Albumin Nanoparticles: Physical Properties. *Pharmaceutical Frontiers*. 1, e190006.
- Papadimitriou, S., Bikiaris, D., Avgoustakis, K., Karavas, E., Georgarakis, M. 2008. Chitosan nanoparticles loaded with dorzolamide and pramipexole. *Carbohydrate Polymers*, 73(1):44–54.
- Patel, R., Gajra, B. 2016. Ganciclovir Loaded Chitosan Nanoparticles: Preparation and Characterization. *Journal of Nanomedicine & Nanotechnology*, (06):7–7.
- Piacentini, E. 2016. Encapsulation Efficiency. In ., D. E., ., G. L., editors, *Encyclopedia of Membranes*, pages 26–72. Springer.
- Popova, M., Trendafilova, I., Zgureva, D., Kalvachev, Y., Boycheva, S., Tušar, N. N., Szegedi, A. 2018. Polymer-coated mesoporous silica nanoparticles for controlled release of the prodrug sulfasalazine. *Journal of Drug Delivery Science and Technology*, 44:415–420.
- Qi, L., Xu, Z., Jiang, X., Hu, C., Zou, X. 2004. Preparation and antibacterial activity of chitosan nanoparticles. *Carbohydrate Research*, 339(16):2693–2700.
- Rampino, A., Borgogna, M., Blasi, P., Bellich, B.,

- Cesàro, A. 2013. Chitosan nanoparticles: Preparation, size evolution, and stability. *International Journal of Pharmaceutics*, 455(1-2):219–228.
- Ray, M., Pal, K., Anis, A., Banthia, A. K. 2010. Development and Characterization of Chitosan-Based Polymeric Hydrogel Membranes. *Designed Monomers and Polymers*, 13(3):193–206.
- Schroeder, K. W., Tremaine, W. J., Ilstrup, D. M. 1987. Coated Oral 5-Aminosalicylic Acid Therapy for Mildly to Moderately Active Ulcerative Colitis. *New England Journal of Medicine*, 317(26):1625–1629.
- Shevchenko, E. V., Talapin, D. V., Kotov, N. A., O'Brien, S., Murray, C. B. 2006. Structural diversity in binary nanoparticle superlattices. *Nature*, 439(7072):55–59.
- Sninsky, C. A. 1991. Oral Mesalamine (Asacol) for Mildly to Moderately Active Ulcerative Colitis. *Annals of Internal Medicine*, 115(5):350–350.
- Soliman, A. A., Mohamed, G. G., Hosny, W. M., El-Mawgood, M. A. 2005. Synthesis, Spectroscopic and Thermal Characterization of New Sulfasalazine Metal Complexes. *Synthesis and Reactivity in Inorganic, Metal-Organic, and Nano-Metal Chemistry*, 35(6):483–490.
- Tavakol, M., Vasheghani-Farahani, E., Hashemi-Najafabadi, S. 2013. The effect of polymer and CaCl₂ concentrations on the sulfasalazine release from alginate-N,O-carboxymethyl chitosan beads. *Progress in Biomaterials*, 2(1):10–10.
- Taylor, K. M., Irving, P. M. 2011. Optimization of conventional therapy in patients with IBD. *Nature Reviews Gastroenterology & Hepatology*, 8(11):646–656.
- Tiyaboonchai, W. 2003. Chitosan Nanoparticles : A Promising System for Drug Delivery. *Naresuan University Journal*, 11(3):51–66.
- Tsai, M., Bai, S., Chen, R. 2008. Cavitation effects versus stretch effects resulted in different size and polydispersity of ionotropic gelation chitosan-sodium tripolyphosphate nanoparticle. *Carbohydrate Polymers*, 71(3):448–457.
- Vino, A. B., Ramasamy, P., Shanmugam, V., Shanmugam, A. 2012. Extraction, characterization, and in vitro antioxidative potential of chitosan and sulfated chitosan from Cuttlebone of *Sepia aculeata* Orbigny, 1848. *Asian Pacific Journal of Tropical Biomedicine*, 2(1):60184–60185.
- Wang, W., Zhu, R., Xie, Q., Li, A., Xiao, Y., Li, K., Liu, H. 2012. Enhanced bioavailability and efficiency of curcumin for the treatment of asthma by its formulation in solid lipid nanoparticles. *International Journal of Nanomedicine*, 7:3667–3677.
- Yi, H., Wu, L. Q., Bentley, W. E., Ghodssi, R., Rubloff, G. W., Culver, J. N., Payne, G. F. 2005. Biofabrication with Chitosan. *Biomacromolecules*. 6(6):2881–2894.
- Younes, I., Rinaudo, M. 2015. Chitin and Chitosan Preparation from Marine Sources. Structure, Properties, and Applications. *Marine Drugs*, 13(3):1133–1174.